Journal of Power Sources 195 (2010) 5862–5867

Contents lists available at ScienceDirect

Journal of Power Sources

journal homepage: www.elsevier.com/locate/jpowsour

# Preparation of catalyst for a polymer electrolyte fuel cell using a novel spherical carbon support

Mika Eguchi[a,*], Atsuhiko Okubo[a], Shun Yamamoto[b], Mayuko Kikuchi[c], Katsuhiro Uno[d], Yoshio Kobayashi[a], Mikka Nishitani-Gamo[c], Toshihiro Ando[e]

[a] Department of Biomolecular Functional Engineering, Faculty of Engineering, Ibaraki University, 4-12-1, Nakanarusawa, Hitachi, Ibaraki 316-8511, Japan
[b] Material and Biological Sciences, Graduate School of Science and Engineering, Faculty of Engineering, Ibaraki University, 4-12-1, Nakanarusawa, Hitachi, Ibaraki 316-8511, Japan
[c] Department of Applied Chemistry, Faculty of Engineering, Toyo University, 2100 Kujirai, Kawagoe, Saitama 350-8585, Japan
[d] Department of Media and Telecommunications Engineering, Faculty of Engineering, Ibaraki University, 4-12-1, Nakanarusawa, Hitachi, Ibaraki 316-8511, Japan
[e] National Institute for Materials Science, 1-1 Namiki, Tsukuba, Ibaraki 305-0044, Japan

ARTICLE INFO

*Article history:*
Received 13 October 2009
Received in revised form
21 December 2009
Accepted 1 January 2010
Available online 13 January 2010

*Keywords:*
Carbon nanofiber
PEFC
Pt
Catalyst supports
TEM
Cyclic voltammetry (CV)

ABSTRACT

In this study, the support Pt catalyst was supported by a novel spherical carbon using a convenient technique. Two different preparation methods utilizing a nanocolloidal solution method without heat treatment were developed (methods 1 and 2). The scanning electron microscope (SEM) and transmission electron microscope (TEM) observations showed that the Pt nanoparticles (particle size) were supported, with higher dispersion being achieved with method 2 than method 1. The peak of the Pt metal was confirmed from the X-ray diffraction (XRD) measurement. Based on the inductively coupled plasma mass spectrometry (ICP-MS) measurements, Pt loading was 19.5 wt.% in method 1 and approximately 50 wt.% in method 2. The Pt specific surface area of the Pt/novel spherical carbon catalyst calculated from the cyclic voltammetry (CV) measurement result was larger than that of the commercially available Pt/Ketjen catalyst. These results indicated that the Pt nanoparticles were supported in high dispersion without heat treatment using novel spherical carbon as a carbon support.



## 1. Introduction

Pt support carbon catalyst (Pt/carbon) of the particulate is used as a catalyst for polymer electrolyte fuel cells (PEFCs). The catalyst layer using Pt support carbon catalyst (Pt/C) is an aggregate structure, the main components of which are an ionomer, which is an electrolyte to move the ion, and vacant space, which the reactant gas passes through. It has been determined that there is a proper value for the ratio between the ionomer and the catalyst [1]. We suggested the catalyst layer element constitutional diagram that consists of each volume ratio of the catalyst, the ionomer, and the vacant space to relate the catalyst layer structure to the cell performance, and demonstrated the utility [2]. It was found that an efficient region disappeared for defective diffusion with the generation water in the high current density region of 1 A $cm^{-2}$ or more at the catalyst with the carbon particle as a support [2].

Recently, to eliminate the problems of defective diffusion of generated water, the use of carbon nanofibers, for example, carbon nanotubes (CNTs) as a catalyst support material with repellency has been investigated. The CNTs have a linear structure. In addition, because electron conductivity, oxidation stability, and the specific surface area are high, CNTS are suitable for use as a fuel cell catalyst. It is expected that a catalyst layer using CNTs would have high gas diffusion compared with a catalyst layer in an aggregate structure using particulate carbon support. In the conventional method for preparing the metal catalyst support [3,4], both acid treatment of the CNTs and heat treatment in the Pt support are necessary [5]. Boennemann et al. have reported a technique for supporting Pt with Vulcan at low temperatures using a colloidal solution [6].

In the present study, we have developed an extremely easy method for preparing a Pt support without acid or heat treatment. We have developed a high-performance electrode catalyst for PEFC to support platinum as a metal catalyst by using the metallic nanocolloidal solution method. An improvement on the nanocolloidal solution method [7–10] is suggested, and catalyst preparation was carried out by both the original and the improved upon methods. A novel spherical carbon that had more hydrophilic properties than CNT was used for the carbon support [11]. While Ketjen and Vulcan known well as a carbon carriers of the fuel cells have structures with inner surfaces, the novel spherical carbon have a structure only with outer surfaces.

* Corresponding author. Tel.: +81 294 38 5086; fax: +81 294 38 5086.
*E-mail address:* eguchi@mx.ibaraki.ac.jp (M. Eguchi).

0378-7753/$ – see front matter © 2010 Elsevier B.V. All rights reserved.
doi:10.1016/j.jpowsour.2010.01.008

**Table 1**
The growth conditions of the spherical carbon.

| | |
|---|---|
| Reactant gas | $CH_4$ |
| | 83% |
| Catalyst | Ni |
| Loading metal weight | 5 wt.% |
| Support material | Oxidized diamond (surface area 12.6 $m^2 g^{-1}$) |
| Reaction temperature | 550 °C |
| Reaction time | 10 h |

## 2. Experimental

### 2.1. Synthesis of the novel spherical carbon

The growth conditions for the novel spherical carbon are shown in Table 1. The oxidized diamond-based catalyst was prepared by impregnating the oxidized diamond into an aqueous solution of metal nitrate. The oxidized diamond was impregnated into an aqueous solution of $Ni(NO_3)_2{\cdot}6H_2O$ and then evaporated under a vacuum condition to prepare the diamond-supported Ni catalyst. The supported catalyst was dried and calcined at 400 °C for 3 h in air prior to the reaction.

The reaction was conducted using a fixed-bed flow-type quartz reactor at atmospheric pressure. $CH_4$ was used as a reactant to obtain the "novel spherical carbon" having different structures. At a temperature of 550 °C, 25 mL $min^{-1}$ of $CH_4$ and 5 mL $min^{-1}$ of Ar were introduced. The reaction time was 10 h.

### 2.2. Catalyst preparation

The flow charts of the two kinds of preparation methods are shown in Fig. 1. Two different preparation methods were used the nanocolloidal solution method (method 1) without heat treatment, and a second method (method 2), which was an improvement on method 1.

The flow charts was shown in Fig. 1 about two methods of the catalyst preparation. Method 1 was a simple combination of the well known two methods [7,11]. After preparation the Pt nanoparticle, the novel spherical carbon was added in method 1. The novel spherical carbon had been added in method 2 before the Pt nanocolloid was generated. Prepared time has been shortened to 1/3 in method 2 compared with method 1.

Method 1 is a metallic nanocolloidal solution method reported by Nagao et al. [7–10]. To prepare the Pt nanocolloidal solution, 0.15 mM NaOH, 0.69 mM citric acid, 0.36 mM $H_2PtCl_6$, and 1.68 mM $NaBH_4$ were added to deionized water and stirred for 1 day. Novel spherical carbon was added to the Pt nanocolloidal solution. At this time, the Pt amount of the Pt nanocolloidal solution was 50 wt.% against the added amount of novel spherical carbon. The nanocolloidal solution with added carbon was stirred for 10 min and then irradiated with an ultrasonic wave for 5 h. The supernatant liquid was removed from the carbon-addition nanocolloidal solution by centrifuge. The solution was then removed from the centrifuge and dried at 80 °C.

Method 2 was an improvement on method 1, and the colloidal solution was prepared with the carbon added first. To prepare the platinum nanocolloidal solution using method 2, 0.15 mM NaOH was added to deionized water, followed by the addition of the novel spherical carbon. The Pt amount of the Pt nanocolloidal solution at this time was 50 wt.% against the added amount of the novel spherical carbon. The carbon-addition solution was stirred for 30 min and then irradiated with an ultrasonic wave for 30 min. Next, 0.69 mM citric acid and 0.36 mM $H_2PtCl_6$ were added to the carbon-addition solution. The solution was stirred for 30 min and then irradiated again by an ultrasonic wave for 30 min. Finally, 1.68 mM $NaBH_4$ was added to the solution. After stirring for 30 min and ultrasonic irradiation for 30 min, the carbon-addition nanocolloidal solution was stirred for 1 day. The supernatant liquid was then removed from the solution by centrifuge, after which the solution was removed from the centrifuge and dried at 80 °C.

### 2.3. Measurement

The morphologies of the carbon products and the loaded Pt metal catalysts were observed by field emission scanning electron microscopy (FE-SEM; Hitachi S-4100, 15 kV). The fine structure of the carbon products and loaded Pt metal catalysts were observed by transmission electron microscopy (TEM; JEOL JEM-2100, 200 kV). Suitable transmission specimens were prepared by ultrasonic dispersion of sections of the carbon products or loaded Pt metal catalysts in methanol and then application of a drop of the resulting suspension to a holey carbon support grid. Prior to examination, the specimens were calcined at 80 °C for 0.5 h.

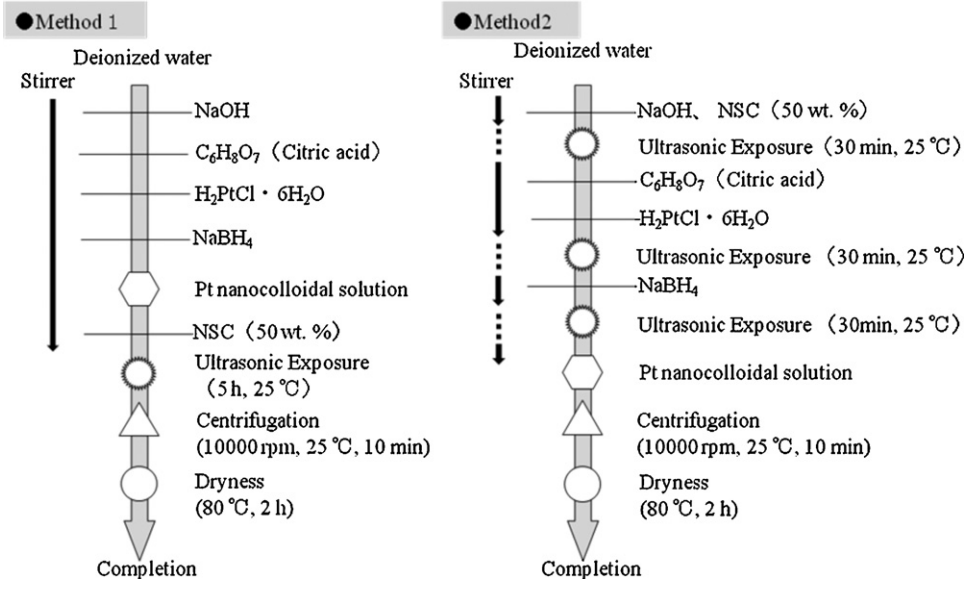


**Fig. 1.** Flow charts of the catalyst preparation.

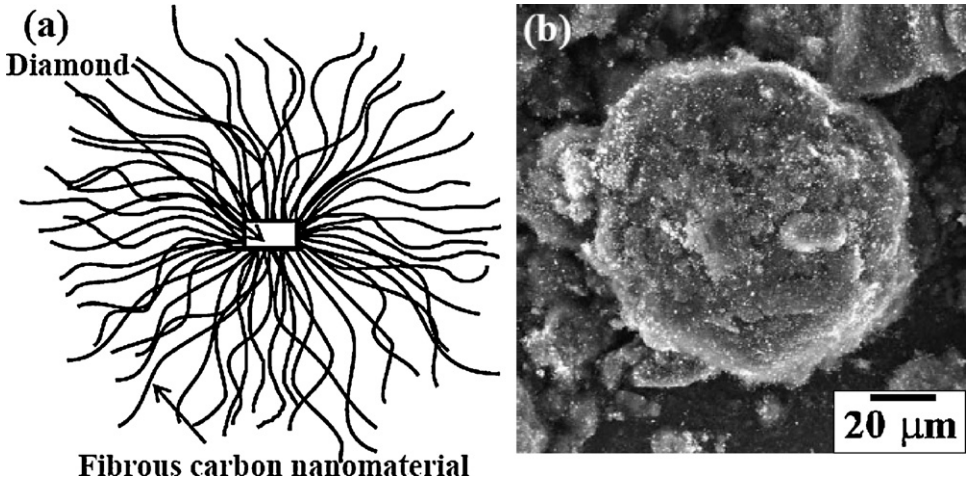


**Fig. 2.** (a) A model of the spherical carbon. (b) SEM image of the spherical carbon.

X-ray diffraction (XRD) measurements (with CuK$\alpha_1$ radiation, RIGAKU RAD-C) was carried out at 25 °C. Catalyst ink (30 μl) was added dropwise on the cross-section of the glassy carbon electrode. The samples obtained were analyzed by powder XRD measurement and confirmed to be a single phase of Pt identified as ICDD card (NO. 4-0802).

The Pt loading was determined by inductively coupled plasma mass spectrometry (ICP-MS) atomic emission spectroscopy with IRIS A advantage (Nippon Jarrell-Ash Co. Ltd.). The Pt loading was calculated based on the remaining Pt concentrations of the catalyst solution and the Pt concentrations of the Pt nanocolloidal solution.

Powder catalysts were applied to the end face of a 5.2-mmϕ glassy carbon. For the powder application, the catalyst was mixed with water. A catalyst ink was stirred with a supersonic wave mixer for 30 min and was applied to the glassy carbon edge. Water was evaporated at 80 °C for 30 min under a nitrogen atmosphere, and the electrode surface was coated with 1% Nafion® solution. Thereafter, it was heat-treated for 30 min at 80 °C and then at 120 °C for 1 h under a nitrogen gas atmosphere, and the catalyst-coated glassy carbon electrode was used for the studies.

A three-electrode cell was used for the electrochemical measurements. The characteristics of the prepared electrode were evaluated by cyclic voltammetry (CV) in a 0.1 M (M = mol dm$^{-3}$) $H_2SO_4$ solution at 30 °C under a nitrogen atmosphere. The reference electrode was a reversible hydrogen electrode (RHE), and the counter electrode was a platinized electrode. The scanning rate was 50 mV s$^{-1}$. The scanning range was 50–1200 mV (vs. RHE) [12].

## 3. Results and discussion

Fig. 2(a) and (b) shows a schematic model and SEM image of the product carbon. The product carbon shows a spherical shape like a "Ball" and is what we refer to herein as the novel spherical carbon. Fine fibrous carbon filaments grew from the point of Ni catalysts on the diamond-support. The initial diamond-supported catalyst particles were covered with the grown carbon nanofilaments. The novel spherical carbon was made of a combination of diamond ($sp^3$ carbon) and fibrous carbon nanomaterial ($sp^2$ carbon). The diamond particle plays the role of the nucleus core in the novel spherical carbon. The fibrous carbon filaments formed by the decomposition of hydrocarbon molecules over nickel particles are dispersed on the diamond-support.

Fig. 3 shows SEM images of the carbon nanofilaments in the novel spherical carbons grown using $CH_4$. The SEM images show that the novel spherical carbon consisted of carbon nanofilaments. The diameters of the carbon nanofilaments were distributed in the range from 40 to 55 nm.

Fig. 4 shows an SEM image of the carbon nanofilaments in the novel spherical carbon-loaded 50 wt.% Pt metal catalyst prepared by method 1. Method 1 produced an aggregation of the Pt parti-

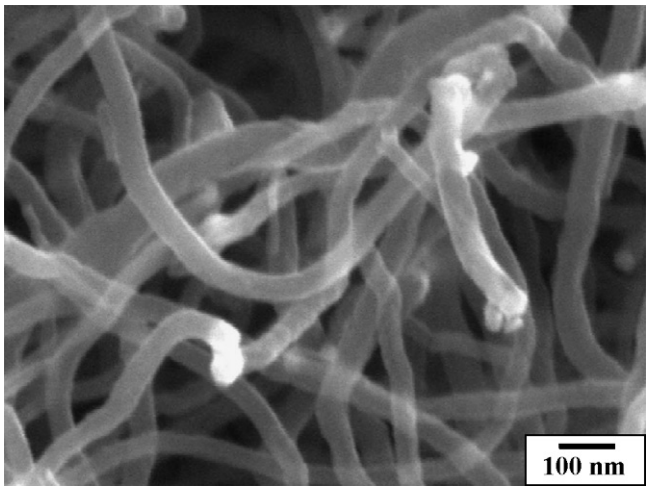


**Fig. 3.** SEM image of the carbon nanofilaments in the spherical carbons.

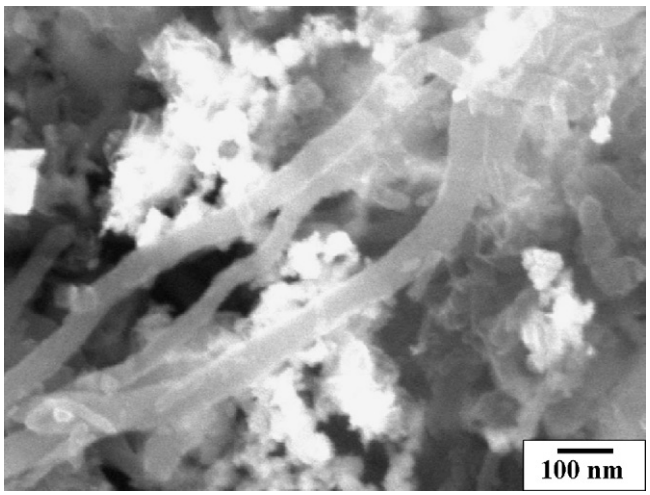


**Fig. 4.** SEM image of the Pt(50 wt.%)/spherical carbon-method 1.

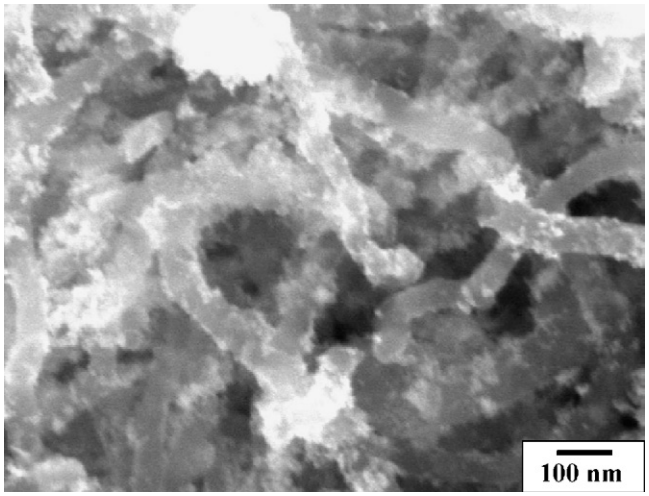


**Fig. 5.** SEM image of the Pt(50 wt.%)/spherical carbon-method 2.

cles. The agglomerated Pt particles were isolated from the carbon nanofilaments.

Fig. 5 shows an SEM image of the carbon nanofilaments in the novel spherical carbon-loaded 50 wt.% Pt metal catalyst prepared by method 2. Method 2 gave a dispersion of Pt nanoparticles. The Pt nanoparticles were dispersively loaded on the carbon nanofilament surfaces. This result was totally different from Fig. 4.

Fig. 6 shows a TEM image of the carbon nanofilaments in the novel spherical carbon-loaded 50 wt.% Pt metal catalyst prepared by method 1. It can be seen here that the Pt particles formed clusters and were not dispersed on the carbon nanofilaments.

Fig. 7 shows TEM images of the carbon nanofilaments in the novel spherical carbon-loaded 50 wt.% Pt metal catalyst prepared by method 2. Fig. 7(a) shows a general representation of the catalyst, in which it can be seen that the Pt nanoparticles were dispersed on the carbon nanofilament surfaces. Each of the deposited Pt nanoparticles could be individually recognized on the carbon nanofilaments. The method 2 realized a dispersive loading of the Pt nanoparticles on the carbon nanofilament surface. The Pt particles ware not directly loaded on the surface of the carbon nanofilaments in the result by method 1 as shown in Fig. 5. In Fig. 7, the Pt particles of 5–8 nm were individually loaded on the surface of the carbon nanofilaments. This result was different from Fig. 5. Fig. 7(b) provides a high-magnification view of the square frame in Fig. 7(a). Pt nanoparticles were loaded edge of graphene sheets. It was like embedded in the space between the graphene sheets. The graphene

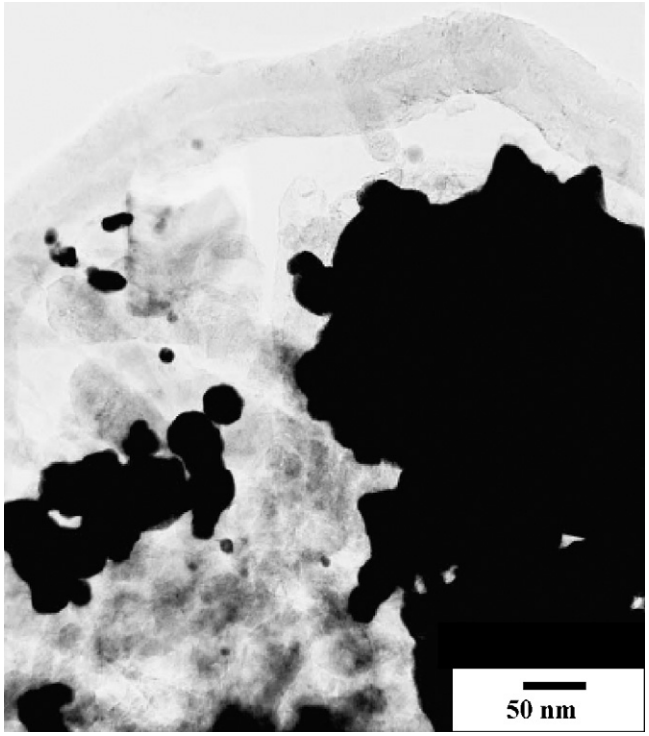


**Fig. 6.** TEM image of the Pt(50 wt.%)/spherical carbon-method 1. (b) is the high-magnification TEM image of (a).

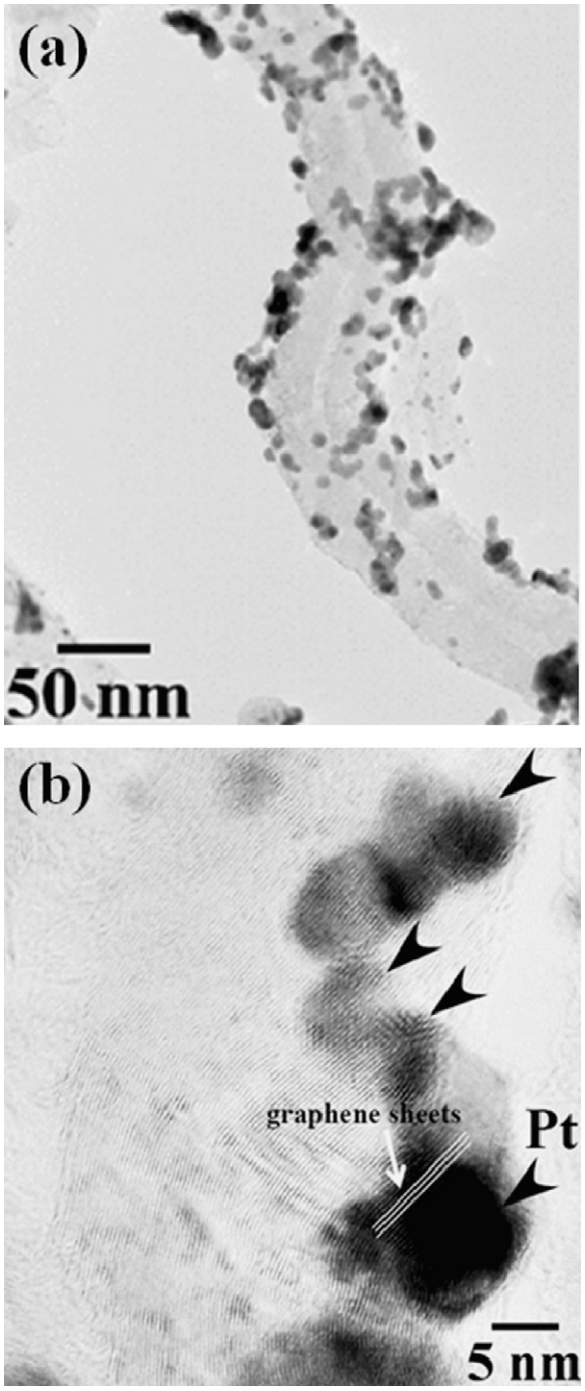


**Fig. 7.** TEM image of the Pt(50 wt.%)/spherical carbon-method 2. (b) is the high-magnification TEM image of (a). (c) is the high-magnification TEM image of the square frame of (b).

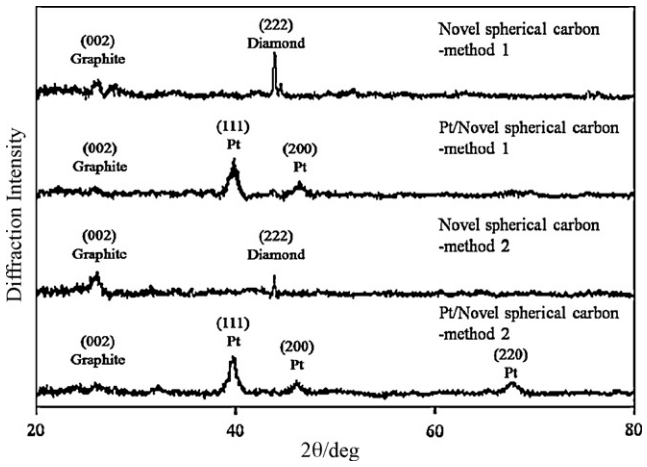


**Fig. 8.** XRD patterns of Pt(50 wt.%)/spherical carbon.

sheets consist of carbon nanofilaments in the novel spherical carbon exposure to surface of carbon nanofilaments. This fine structure of the novel spherical carbon resulted in the existence of Pt ions on the edges of the graphene sheets. Nucleation of these Pt ions then occurred. Finally, Pt nanocolloids may be generated at the same location. We revealed that the method 2 is effective in dispersed loading of the Pt nanoparticles on the carbon nanofilaments.

The XRD diffraction profiles of novel spherical carbon (upper row) and Pt/novel spherical carbon (the lower) are shown in Fig. 8. A diffraction peak for Graphite (0 0 2) was observed, as shown in Fig. 8. The diffraction peak for the metallic platinum can be observed by the XRD profile of Pt/novel spherical carbon. These results suggest that the metallic platinum is being supported in the novel spherical carbon.

The ICP-MS results are shown in Table 2. The Pt amount in the Pt/novel spherical carbon was approximately 19.5 wt.% in method 1 and 50 wt.% in method 2, respectively. Because many of the Pt nanoparticles in method 2 were supported by the novel spherical carbon compared with method 1, based on the TEM observations, the amount of Pt in method 2 was large. As also seen in Table 2, Fe and Ni are catalysts for the growth of the novel spherical carbon.

The cyclic voltammetry curves of the catalysts prepared by method 1 and 2 are shown in Fig. 9. In the catalysts prepared by methods 1 and 2, hydrogen adsorption and desorption peaks were observed in the region of 0.055–0.4 V, and oxygen adsorption and desorption peaks were observed in the region of 0.9–1.2 V. These peaks show that hydride and oxygenate films existed on the Pt surface. The peaks on the low potential side are characteristic Pt peaks that show an ideal surface state onto which the atomic Pt is arranged and ordered. The plateau observed over the range of 0.3–0.6 V depends on the formation of an electrical double layer consisting of both an immobile layer and a diffusion layer on the electrode surface. A physical surface area of the spherical carbon of method 1 and 2 and Pt/Ketjen in the BET measurement was 75.4, 76.7, and 294 $m^2\ g^{-1}$, respectively, as shown in Table 3. The some part of the BET surface area of Ketjen is a surface area of the internal pore. The spherical carbon is an outer surface structure, and doesn't have the internal pore. Therefore, the BET surface area of the spherical carbon was about 1/5 of the BET surface areas of Ketjen. The values of the active surface area of Pt calculated from the hydrogen adsorption peak area of the CV-curve are shown in Table 3, and the calculation formula for the active surface area of Pt is as follows:

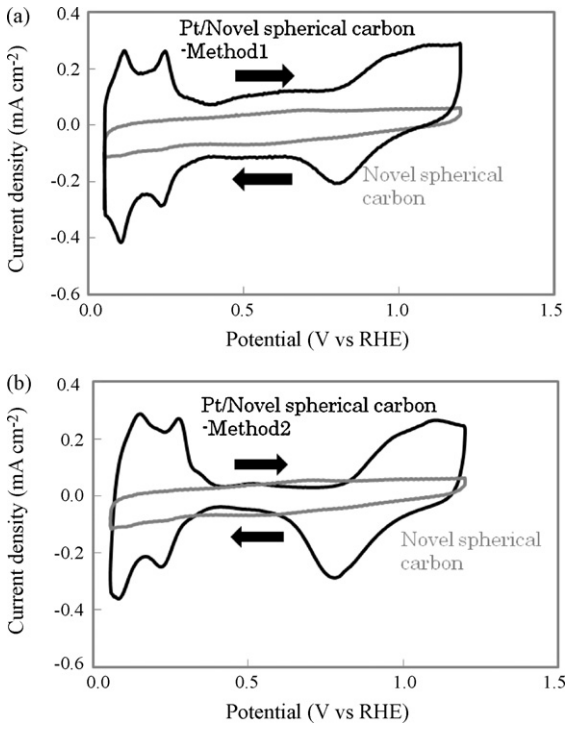


**Fig. 9.** Cyclic voltammogram of Pt(50 wt.%)/spherical carbon.

$$\frac{\text{Hydrogen adsorption quantity of charge}\ (\mu C)}{210\ (\mu C)} \times \frac{1}{\text{Pt weight}\ (g)} = \text{r.s.a}\ (m^2\ g^{-1}) \quad (1)$$

The quantity for the charge of adsorption for each Pt unit surface area is 210 μC [13,14]. The Pt surface area was calculated by dividing the charge quantity of the hydrogen adsorption by 210 μC. In addition, the specific active surface area for each gram of Pt supported on the electrode was calculated. The Pt surface areas in methods 1 and 2, as well as in commercially available Pt/Ketjen as a comparison, were 4.21 $cm^2$, 5.28 $cm^2$, and 1.26 $cm^2$, respectively. In method 1, the effect of the nanocolloidal solution method was not seen. It is thought that the Pt nanoparticles could not move into the interior of the novel spherical carbon in the state of the Pt colloid. However, in method 2, because the colloidal state was formed on the surface of the novel spherical carbon, the Pt surface area of method 2 was approximately four times greater than that of the surface area of Pt/Ketjen. The Pt specific active surface areas in methods 1 and 2 as well as that of Pt/Ketjen were 32.8 $m^2\ g^{-1}$, 105.5 $m^2\ g^{-1}$, and 22.4 $m^2\ g^{-1}$, respectively. The Pt

**Table 2**
ICP data of Pt(50 wt.%)/spherical carbon.

| Element | Novel spherical carbon-method 1 (wt.%) | Novel spherical carbon-method 2 (wt.%) |
|---|---|---|
| Pt | 19.5 | 50 |

**Table 3**
Surface area, specific surface area and BET of Pt(50 wt.%)/spherical carbon.

| | Surface area ($cm^2$) | Specific surface area ($m^2\ g^{-1}$) | BET ($m^2\ g^{-1}$) |
|---|---|---|---|
| Pt/novel spherical carbon-method 1 | 4.21 | 32.8 | 75.4 |
| Pt/novel spherical carbon-method 2 | 5.28 | 105.5 | 76.7 |
| Pt/Ketjen | 1.26 | 22.4 | 294 |

specific active surface areas in methods 1 and 2 were greater than those obtained with Pt/Ketjen. It was conjectured that the novel spherical carbon creates a carbon support that can more easily support Pt.

## 4. Conclusion

The Pt nanoparticles were supported by novel spherical carbon as a result of two different preparation methods that improved upon the metallic nanocolloidal solution method, making water treatment of the carbon support and heat treatment unnecessary. Method 1 was a simple combination of the well known method. After preparation the Pt nanoparticle, the novel spherical carbon was added in method 1. The novel spherical carbon had been added in method 2 before the Pt nanocolloid was generated. Prepared time has been shortened to 1/3 in method 2 compared with method 1. The characteristics of these catalysts characteristics were then investigated. SEM and TEM observations showed that the Pt nanoparticles were supported by the novel spherical carbon. In the catalyst prepared by method 1, a part of the Pt nanoparticles had agglomerated. In contrast, the Pt nanoparticles were supported by high dispersion in the catalyst prepared by method 2. Therefore, it was revealed that the support state of the Pt nanoparticles is influenced by the catalyst preparation procedure. It appears to be effective for the carbon support to be added before the Pt colloid is prepared. It was revealed that the catalyst prepared by method 2 has higher catalytic activity than that prepared by method 1, based on use of a fixed quantity of Pt by ICP-MS, as well as an effective Pt surface product, based on the CV measurement. In addition, the BET surface area of the spherical carbon was about 1/5 of the BET surface areas of Ketjen, while the catalyst prepared by using novel spherical carbon showed higher catalytic activity than the catalyst of commercially available Ketjen. Novel spherical carbon showed high catalytic activity as a catalyst for polymer electrolyte fuel cells.

## Acknowledgements

The authors are grateful to T. Aoki for his technical assistance in TEM observation. This work was financially supported in part by Toppan Printing Co., Ltd.

## References

[1] P. Staiti, Z. Poltarzewski, V. Alderucci, G. Maggio, N. Giordano, Int. J. Hydrogen Energy 19 (1994) 523–527.
[2] K. Uno, M. Eguchi, T. Suzuki, Y. Tsutsumi, J. Surf. Finish. Soc. Jpn. 60 (2009).
[3] T. Onoe, S. Iwamoto, M. Inoue, Catal. Commun. 8 (2007) 101–105.
[4] T. Matsumoto, T. Komatsu, H. Nakano, K. Arai, Y. Nagashima, E. Yoo, T. Yamazaki, M. Kijima, H. Shimizu, Y. Takasawa, J. Nakamura, Catal. Today 90 (3–4) (2004) 277–281.
[5] C.A. Bessel, K. Laubernds, N.M. Rodriguez, R. Terry, K. Baker, J. Phys. Chem. B 105 (2001) 1115–1118.
[6] H. Boennemann, R. Binkmann, P. Britz, U. Endruschat, R. Moertel, U.A. Paulus, G.J. Feldmeyer, T.J. Schmidt, H.A. Gasteiger, R.J. Behm, J. New Mater. Electrochem. Syst. 3 (2000) 199.
[7] Y. Shimazaki, Y. Kobayashi, S. Yamada, T. Miwa, M. Konno, J. Colloid Interface Sci. 292 (2005) 122–126.
[8] D. Nagao, Y. Shimazaki, Y. Kobayashi, M. Konno, Colloids Surf. A: Physiochem. Eng. Aspects 273 (2006) 97–100.
[9] Y. Shimazaki, Y. Kobayashi, M. Sugimasa, S. Yamada, T. Itabashi, T. Miwa, M. Konno, J. Colloid Interface Sci. 300 (2006) 253–258.
[10] D. Nagao, Y. Shimazaki, S. Saeki, Y. Kobayashi, M. Konno, Colloids Surf. A: Physiochem. Eng. Aspects 302 (2007) 623–627.
[11] K. Nakagawa, H. Oda, A. Yamashita, M. Okamoto, Y. Sato, H. Gamo, M. Nishitani-Gamo, K. Ogawa, T. Ando, J. Mater. Sci. 44 (2009) 221–226.
[12] Electrochemical Society of Japan (Ed.), The Basic Manual of Electrochemistry Measurement, MARUZEN Co. Ltd., 2002, pp. 74–94.
[13] T. Biegler, D.A.J. Rand, R. Woods, Electroanal. Chem. Interface Electrochem. 29 (1971) 269–277.
[14] V.S. Bagotzky, Y.B. Vassilyev, Electrochem. Acta 12 (1967) 1323–1343.